

THERMAL BEHAVIOR OF MASS CONCRETE STRUCTURES WITH DIFFERENT MATERIAL PROPERTIES

Trong Chuc Nguyen^{1,*}, Kim Dien Vu², Van Sang Dau¹

¹Le Quy Don Technical University, Hanoi, Vietnam;

²College of Industry and Construction, Quang Ninh, Vietnam

Abstract

In mass concrete constructions, cement hydration produces much heat at an early age. Because of the different distribution of temperature in their parts, which leads to a significant temperature difference between the concrete block's center and outer surface. When the temperature difference among structural parts surpasses the permissible temperature difference, thermal cracks can occur. Hence, this article presents the development of the temperature field in mass concrete structures with two different concrete mixes M_1 and M_2 . M_1 consists of 100% ordinary Portland cement, and M_2 consists of 65% ordinary Portland cement and 35% fly ash. Furthermore, by using the finite element method, the effect of the initial temperature of concrete mixtures (M_1 , M_2) on the temperature field in the structure has been investigated. The researched results can be used to reduce the risk of thermal crack formation in mass concrete.

Keywords: Crack formation; temperature regime; compressive strength; tensile strength; maximum temperature.

1. Introduction

Mass concrete has been developed and popularly used in various infrastructure projects, such as foundations, bridges, ports, and dams [1]. However, cracks formation in concrete structures due to increased hydration of cement exist the problem. One of the main causes of the formation of thermal cracks at an early age is the increased temperature of the hydration of the cement and moisture changes during the hardening of concrete. The temperature of the concrete mass increases during curing and is formed as a result of the chemical reaction between the minerals of the cement and water. After Portland cement is mixed with water, heat is radiated, which heat has been defined as the heat of hydration [2-4]. The concrete structure with its small size, this heat escapes relatively quickly and does not cause cracking problems. In concrete structures of large size, due to the poor thermal conductivity of concrete, a high-temperature difference may occur between the center and the surface of concrete structures. Concrete structures

* Email: trongchuc.nguyen@lqdtu.edu.vn

curing is accompanied by a moisture exchange when the ambient temperature changes. The evaporation of water at the surface of concrete structures results in shrinkage, which is defined as an external drying shrinkage [5]. Besides, the loss of water internal in concrete mass results from the reduction in material volume as water is consumed by hydration, which is defined as autogenous shrinkage. The volume changes due to rising temperature and moisture transformation have resulted in formation stresses in the concrete structures. When the tensile stress exceeds the tensile strength of the concrete cracks can be formed in the concrete structure. So, it is necessary to have significant efforts to control maximum temperature due to the heat of hydration of the cementations' materials. The temperature field in mass concrete at early age depends on many factors such as the intensity of concreting, cement content in 1 m³ of concrete, type of cement, the initial temperature of the concrete mixture, size of concrete block, type of formwork, air temperature, etc. [6-8].

Effective solutions are necessary to control the maximum temperature created by the process of cement hydration in concrete mass include the following: (i) adjustment in the concrete mix by replacing the cement material by generating materials less heat; (ii) reducing the fresh mix temperature of the concrete; (iii) using aggregates with low thermal expansion; (iv) using the cooling pipe system and controlled curing water temperature; (v) reducing temperature difference in mass concrete by surface insulation, etc. [9-11].

The article presents the development of temperature fields in mass concrete with two different concrete mixes combined to evaluate the effect of their initial temperature. The research results can be used for controlling the risk of forming thermal cracks to suit construction conditions.

2. Materials and methods

2.1. Materials

Quartz sand, fly ash, stone and Portland cement were used as raw materials.

Ordinary Portland Cement (OPC) was produced by the Tam Diep plant (Vietnam) with a density of 3.14 g/cm³. The analysis results of the used Portland cement are shown in Tab. 1 and Tab. 2.

Tab. 1. Mineralogical composition, physical and mechanical properties of Tam Diep Portland cement

Mineral composition (%)					Time of setting (min)		Compressive strength (MPa)			Standard consistency (%)
C ₃ S	C ₂ S	C ₃ A	C ₄ AF	Other	Initial	Final	3 days	7 days	28 days	
56.15	22.47	5.14	12.25	3.99	142	235	35.1	40.4	52.3	29.5

Tab. 2. Chemical compositions and physical properties of Portland cement and fly ash

Chemical components (wt. %)	Fly ash	Portland cement
SiO ₂	61.22	20.4
Al ₂ O ₃	21.17	4.4
Fe ₂ O ₃	5.85	5.4
SO ₃	2.42	3.4
K ₂ O	1.25	1.2
Na ₂ O	1.23	0.3
MgO	0.57	2.5
CaO	1.12	60.2
P ₂ O ₅	1.03	-
LOI ^(*)	4.14	2.2
Average particle size (μm)	6.15	8.365
Specific gravity (g/cm ³)	2.35	3.14
Dry density (kg/m ³)	575	1250
Surface area (m ² /g)	0.582	0.365

2.2. Object of research

In this study, 3D modeling of the concrete mass has the size of $8 \times 6 \times 3$ (m) and the soil under the concrete mass has the size of $16 \times 12 \times 4$ (m). Because the structure has two-way symmetry in the plan taken of symmetry of two directions of the concrete mass can be idealized as one-quarter of the concrete mass. The number of 2509 elements and 1920 nodes used to simulate the analysis of thermal problems is shown in Fig. 1.

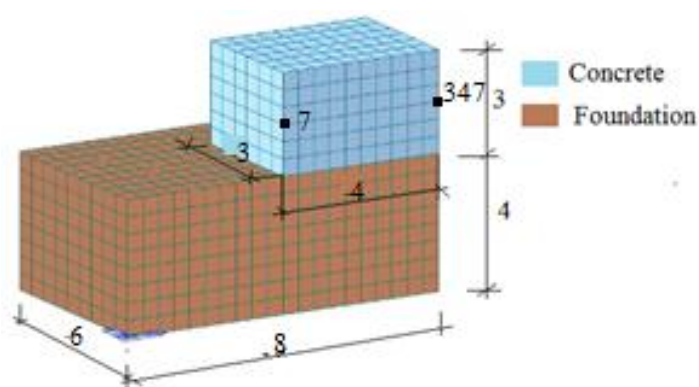


Fig. 1. The finite-element 3D model, unit m.

The temperature difference between the center and the surface of the concrete block is significantly dependent on the convection coefficient and the air temperature. The

convection coefficient of concrete-air can be constant or depends on time and temperature. The convection coefficient was calculated by the following equation [12]:

$$h_c = \begin{cases} 5.6 + 3.95v, & v \leq 5 \text{ m/s} \\ 7.6v^{0.78}, & v \geq 5 \text{ m/s} \end{cases} \quad (1)$$

where v is the wind speed, m/s.

To investigate the effects of placing temperature on the heat of hydration in mass concrete. Four different temperatures at 15°C, 20°C, 25°C and 30°C. To investigate the effects of different compositions of concrete mixtures on the heat of hydration in mass concrete, two different mixtures of concrete with a specified compressive strength of 30 MPa are mixed. Mix 1 consists of 100% ordinary Portland cement; mix 2 consists of 65% ordinary Portland cement and 35% fly ash. The composition of concrete mixtures and the mechanical properties used to describe the strength development over time of the concrete mass are presented in Tab. 3 and Tab. 4.

2.3. Method

To determine the composition of concrete mixes, the absolute volume method is used.

The compressive strength of concrete was determined at the age of 1, 3, 7, 14, and 28 days on cube specimens 150 × 150 × 150 (mm) in size. In this case, the tensile strength of concrete was determined on specimen beams to size 150 × 150 × 600 (mm) at the age of 28 days by the Russian standard GOST 10180-2012. In addition, the elastic modulus of concrete is determined according to ASTM C 469-2002 at 1, 3, 7, 14, and 28 days of age.

The initial ratios of raw materials for the production of concrete were chosen by us as follows: Water/binder = 0.5, Fly ash replaces 35% cement, Quartz sand/binder = 2, Stone/binder = 2.5 (binder = (Cement + Fly ash)). The results of which are presented in Tab. 3.

Tab. 3. Concrete composition

No.	Material, kg/m ³				
	Cement	Fly ash	Water	Quartz sand	Stone
M ₁	398	0	199	797	996
M ₂	287	135	194	774	968

Heat is generated by the products of chemical reactions during the hydration of Portland cement and water after Portland cement is mixed with water. The process is known as hydration. Hydration heat is a very important factor because it is used as the source of heat in concrete mass. The hydration power of the two cementations mixture is shown in Fig. 2 [13].

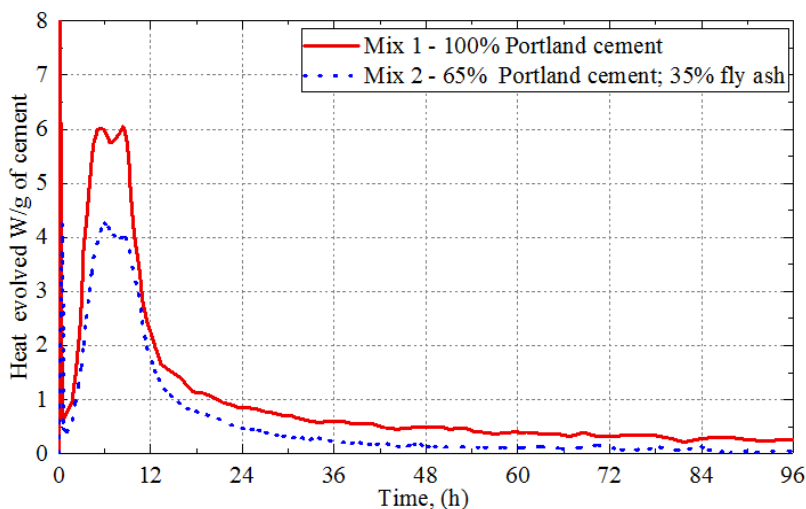


Fig. 2. Hydration power of two cementitious mixture.

Important parameters of concrete and foundation used to model finite elements are shown in Tab. 4.

Tab. 4. Important parameters of concrete and foundation

Important parameters	Concrete	Foundation
Thermal conductivity coefficient, λ [W/(m.°C)]	2.9	2.1
Specific heat, c [kJ/(kg.°C)]	1.12	0.85
Specific weight, ρ [kg/m ³]	2400	2600
Elastic modulus, E [MPa]	$E(t)$	13
Coefficient of thermal expansion, 1/°C	1×10^{-5}	1×10^{-5}
Poisson's ratio	0.2	0.3

2.4. Finite element method to solve the thermal model

The heat transfer equation is expressed by the equation [13-15]:

$$k \left(\frac{\partial^2 T}{\partial x^2} + \frac{\partial^2 T}{\partial y^2} + \frac{\partial^2 T}{\partial z^2} \right) + q_v = \rho c \frac{\partial T}{\partial t} \quad (2)$$

where k is thermal conductivity $k = \lambda^2/c \cdot \rho$, m²/s; λ is the thermal conductivity of materials, W/m°C; q_v is the rate of thermal energy generated per unit volume, J/(m³.s); c is specific heat, kJ/(kg.°C); ρ is density, kg/m³; t is age of concrete at the time, day.

To solve equation (2) it is necessary to use the thermal boundary condition given by equation (3):

$$k \left(\frac{\partial T}{\partial x} n_x + \frac{\partial T}{\partial y} n_y + \frac{\partial T}{\partial z} n_z \right) + q_c = 0 \quad (3)$$

where n is vector perpendicular to the direction of heat transfer, q_c is the heat transfer rate per unit area.

Using above mentioned models and equations to analyze the hydration heat of mass concrete by software Midas civil with the basic structural members and the maximum temperature of the center. The maximum tensile strength of the end and crack index was investigated.

The relationship between the hydration heat of cement and the age of concrete can be represented by the equation [16]:

$$Q(t) = Q_0(1 - e^{-mt}) \quad (4)$$

where $Q(t)$ is the cumulative heat of hydration of cement per unit weight of cement J/kg at the age of t day, Q_0 is the total heat of hydration and m is a value related to testing of cement and curing temperature usually gets $m = 0.83$ [17].

The finite element method to solve the problem of heat transfer is expressed by equations as matrix written abbreviated as follows [18, 19]:

$$[K]\{T\} + [C]\left\{\frac{\partial T}{\partial t}\right\} = [Q] \quad (5)$$

Time analysis into steps Δt is as follows:

$$\left\{\frac{\partial T}{\partial t}\right\} = \frac{1}{\Delta t} [\{T(t_n) - T(t_{n-1})\}] \quad (6)$$

Equation (5) can be rewritten as follows:

$$[K]\{T\} + \frac{[C]}{\Delta t} [\{T(t_n) - T(t_{n-1})\}] = [Q] \quad (7)$$

where $[K]$ is stiffness matrix, $[C]$ is capacity matrix, $[Q]$ is thermal load vector, $\Delta t = \Delta t_n - \Delta t_{n-1}$ are steps of computation time.

Validation and numerical application: The temperature fields and stress fields have been analyzed in a finite element method algorithm developed to study 2D and 3D heat transients in a homogeneous isotropic material. The finite element method code can perform the stress-strain analysis for the problem 2D or 3D, both in stationary or dynamic thermal conditions as well as a full three-dimensional stress analysis. Many results of previous studies were compared with experimental results with acceptable errors [18, 20, 21].

3. Results and discussion

3.1. Mechanical properties of concrete

The mechanical properties of concrete such as compressive strength, tensile strength, and elastic modulus are given in Tab. 5.

Tab. 5. Mechanical properties of concrete

Mechanical properties		Day				
		1	3	7	14	28
M ₁	Modulus of elasticity, GPa	13.43	18.12	20.21	22.24	26.17
	Compressive strength, MPa	45.69	57.35	61.56	62.53	63.58
	Tensile strength, MPa	1.25	1.93	2.21	2.97	3.55
M ₂	Modulus of elasticity, GPa	9.78	14.46	16.52	18.87	24.21
	Compressive strength, MPa	29.68	33.81	43.52	48.31	53.64
	Tensile strength, MPa	0.67	1.28	1.63	1.91	3.23

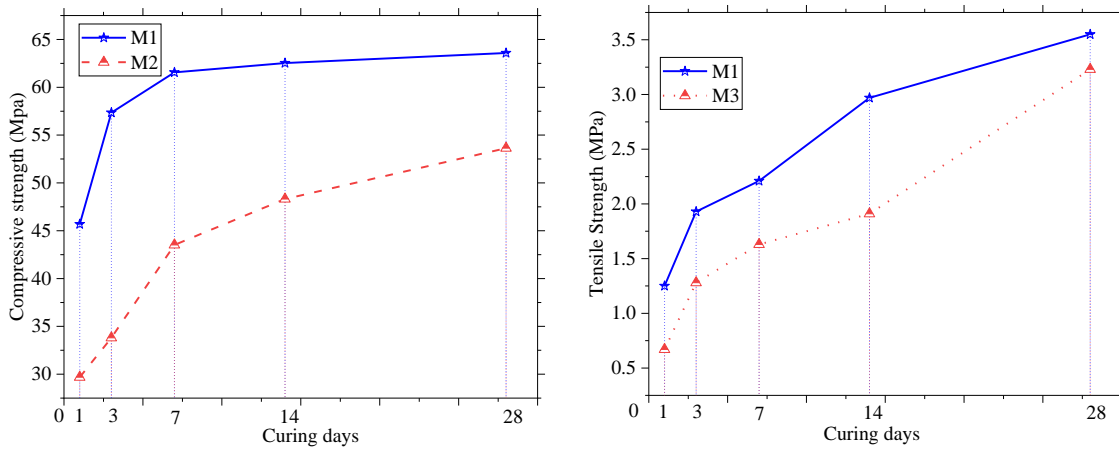


Fig. 3. Effect of fly ash on concrete strength development.

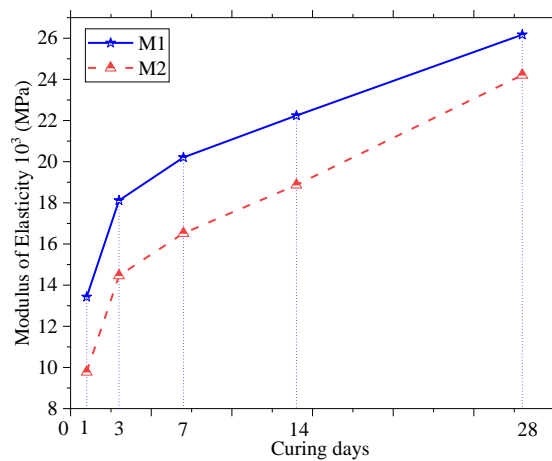


Fig. 4. Effect of fly ash on the concrete elastic modulus.

From Figures 3, 4 we see that:

The development of compressive strength, tensile strength and elastic modulus of concrete always increase with age. The mechanical properties of concrete containing 35% fly ash (M_1) instead of cement are always lower than concrete containing 100% (M_1) cement. Besides, the results showed that the compressive strength at 7 days of the control using 100% cement increased significantly specifically 61.56 MPa while in the samples using fly ash, the compressive strength at 7 days of age develops slowly. Specifically, the rate of replacement fly ash is 35%, and the compressive strength is 43.52 MPa. This is because at the early stage of hydration, the pozzolanic reaction of fly ash is slower than that of cement. Concrete samples using 100% PC cement have early development compressive strength, the strength at 7 days has increased significantly, much higher than samples using fly ash instead of cement. However, at the age of 28 days, the slope coefficient between the 2 samples is not much different and tends to be closer together. This means that, at a period of 28 days, the compressive strength of the concrete using 100% of the cement and 35% of the fly ash replacing the cement has a low difference, the fly ash makes the concrete grow in strength 7 days slowly at an early stage and slowly develop in later stages.

3.2. Thermal behavior of mass concrete structures with different material properties

Placing temperature has an important effect on the hydration process of concrete mass in the early day. Effects of placing temperature of concrete on the concrete hardening temperatures for two different types of mixed concrete at 15°C, 20°C, 25°C, and 30°C are shown in Fig. 5.

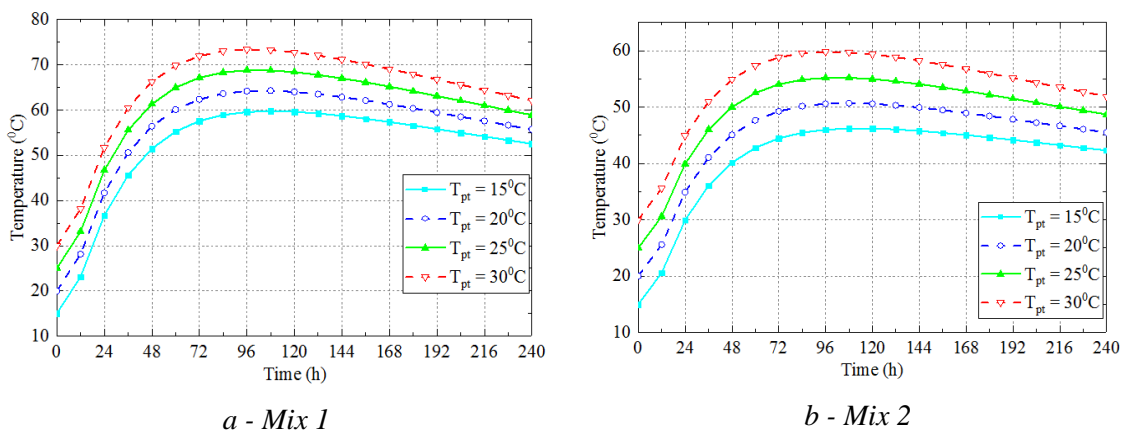


Fig. 5. Temperature development at the center of the concrete mass.

Figure 5 shows the temperature development at the center of concrete blocks with different concrete mixes. As can be seen in Fig. 5, after the concrete placement, the temperature at the center of the concrete block increases to the maximum temperature value and then decreases with time. It can be seen that, with the concrete mix M1, the maximum temperature increases from 60.05°C to 73.38°C when the initial temperature of the concrete mix increases from 15°C to 30°C. In addition, the maximum temperature in the concrete block with the M2 concrete mixture increases from 45°C to 59.79°C when the initial temperature of the concrete mixture increases from 15°C to 30°C. In addition, it should be noted that reducing the cement content in the concrete mixture significantly reduces the maximum temperature inside a mass concrete. Especially when replacing 35% of the binder with fly ash, the maximum temperature in the concrete block can be reduced by 20% compared to the concrete mix consisting of 100% cement binder.

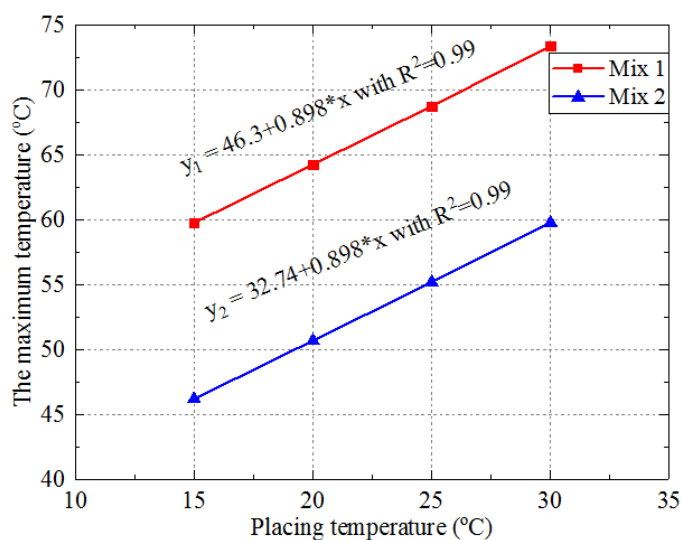


Fig. 6. The relation between placing temperature and the maximum temperature in the concrete mass.

The effect of the placing temperature of concrete mixes on the maximum temperature differentials is presented in Fig. 6. Fig. 6 shows the relationship between the maximum temperature in the mass concrete structure and the initial pouring of concrete mixtures by linear equations:

$$M_1: y_1 = 46.3 + 0.898*x \text{ with } R^2 = 0.99; M_2: y_2 = 32.74 + 0.898*x \text{ with } R^2 = 0.99.$$

From the results, it can be seen that the use of fly ash instead of cement reduces the maximum temperature in mass concrete structures during the hardening of concrete. The maximum temperature difference between the two grades of the concrete mix is 13.56°C for any initial temperature of the concrete mix.

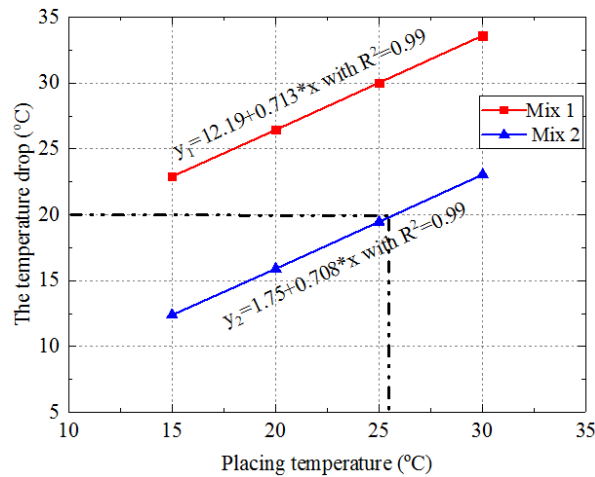


Fig. 7. The relation between placing temperature and the temperature drop in the concrete mass.

Such temperature differences in concrete structures of the cases mixed concrete with different compositions of concrete mixtures are shown in Fig. 7. The effect of the placing temperature of concrete mixes on the temperature difference in mass concrete blocks has linear functions:

$$M_1: y_1 = 12.19 + 0.713*x \text{ with } R^2 = 0.99; M_2: y_2 = 1.75 + 0.708*x \text{ with } R^2 = 0.99.$$

It is worth noting that in a case with mixed concrete M1 the temperature difference between the interior and the surface exceeds 20°C in all the cases of placing temperature of the concrete mixture (Fig. 7). This value is particularly important since many specifications typically limit the maximum temperature difference to 15 ÷ 20°C to limit the difference in volume changes and the likelihood of cracking.

4. Conclusions

Based on the results of the studies, the following conclusions:

- Controlling the risk of thermal-shrinkage cracks occurrence in concrete massive structures is difficult because many materials and technology factors affect the thermal regime in concrete mass in the early days.

- In this study, the impact of the effects of different compositions of concrete mixtures on the concrete hardening temperatures, induced stresses, and the cracking risk in the concrete mass is discussed.

- To reduce the likelihood of crack formation, it is necessary to take appropriate measures. When the model with two mixed concretes (M_1 , M_2) was compared, the maximum temperature structure was reduced in mixed concrete M_2 due to the amount of cement replaced by fly ash. At the same time, the risk of cracking does not occur in mass concrete structures with M_2 concrete mixture when the initial temperature of the concrete mixture does not exceed 25°C.

- From the results, control the risk of thermal cracks in mass concrete early and take measures to prevent cracks to suit building conditions.

Acknowledgments

This study is funded by Le Quy Don Technical University under project number 22.1.71.

References

- [1] Aniskin N., Nguyen T. C., “The thermal stress of roller compacted concrete dams during construction”, *MATEC Web of Conferences*, 196, 04059, 2018. XXVII R-S-P Seminar 2018, Theoretical Foundation of Civil Engineering.
- [2] Aniskin N., Nguyen T. C., “Temperature regime of massive concrete dams in the zone of contact with the base” *IOP Conf. Series: Materials Science and Engineering*, 365, 042083, 2018.
- [3] Aniskin N., Nguyen T. C., Hoang Q. L., “Influence of Size and Construction Schedule of Massive Concrete Structures on its Temperature Regime”, *MATEC Web of Conferences*, 251, 02014, 2018.
- [4] Korea Concrete Institute, *Thermal crack control of mass concrete* (Manual, 2010).
- [5] Zhu B., *Thermal stresses and temperature control of mass concrete*, the United States of America, 2014.
- [6] Kogan E. A. “Rolled-compacted concrete dams: Analysis of foreign data on cracking and recommendations on ensuring the thermal crack resistance”, *Scientific and technical book «Safety of power works»* Issue 6 JSCAO NIIES M, pp. 157-183, 2000.
- [7] *Roller-Compacted Concrete. Design and Construction Considerations for Hydraulic Structures*. U.S. Department of the Interior Bureau of Reclamation Technical Service Center Denver Colorado, 2017, p. 177.

- [8] Tatro Stephen B., Schrader E. K., "Thermal considerations for roller compacted concrete", *Journal of the American Concrete Institute*, 82(2), pp. 119-128, 1985.
- [9] Orod Zarrin Mohsen Ramezan Shirazi, "Roller Compacting Concrete «RCC» in Dams World Academy of Science", *Engineering and Technology International Journal of Civil and Environmental Engineering*, 9(2), 2015.
- [10] Wondwosen A., Girum U., "Numerical prediction model for temperature distribution in concrete at early ages", *American Journal of Engineering and Applied Sciences*, 7(2), pp. 261-271, 2014.
- [11] Tressa Kurian, Kavitha P. E., Bennet Kuriakose, "Numerical analysis of temperature distribution across the cross section of a concrete dam during early age" *American Journal of Engineering and Applied Sciences*, V. 1(2), pp. 26-31, 2013.
- [12] Kuzmanovic V., Savic L., Stefanakos J., "Long-term thermal analysis of RCC dams using 2D and 3D models Canadian", *Journal of Civil Engineering*, 37, pp. 600-610, 2010.
- [13] Nguyen T.C., Dang T.T.H., Nguyen T.S., "Simulation the change of temperature field in structures mass concrete with a content of additives change in cement", *Journal of Science and Technique*, 195(12), pp. 80-88, 2018.
- [14] Ginzburg S. M., Rukavishnikova T. N., Sheinker N. Y., "Simulation models for evaluation of temperature regime of concrete dam", *Bureya HPP Izvestia VNIIG* 241, pp. 173-178, 2002.
- [15] Adler Y. P., Markova E. V., Granovsky Y. V., *Experiment planning in search of optimum conditions*, M.: Nauka, 1976, pp. 70-92.
- [16] Kim J. O., Mueller C. W., *Factor Analysis: Statistical methods and practical issues*, Newbury Park, CA: Sage Publications, 1978.
- [17] Gorsuch, R. L., *Factor Analysis*, Hillsdale, NJ: Lawrence Erlbaum Associates, 1983.
- [18] Rasskazov L. N., Orekhov V. G., Aniskin N. A. and others, *Hydraulic structures in 2 volumes*, M. Publishing House ACB, 2011.
- [19] Zaporozhets I. D., Okorokov S D, Pariysky A. A., *Concrete heat release*, L.: Stroitelstvo, 1966, pp. 99-103.
- [20] ANSYS Mechanical APDL. Documentation. Internet: <http://www.ansys.com> Khovansky G S 1976 Fundamentals of nomograph theory Publishing House «Nauka» chief editors of physical and mathematical publications, Moscow, pp. 217-238.
- [21] Harold Ainsley Evesham, *The History and Development of Nomography of Docent*, Press, 2010, p. 267.

ỨNG XỬ NHIỆT CỦA KẾT CẤU BÊ TÔNG KHỐI LỚN VỚI CÁC ĐẶC TÍNH VẬT LIỆU KHÁC NHAU

Nguyễn Trọng Chức¹, Vũ Kim Diễm², Đậ Văn Sáng¹

¹Đại học Kỹ thuật Lê Quý Đôn, Hà Nội, Việt Nam;

²Trường Cao đẳng Công nghiệp và Xây dựng, Quảng Ninh, Việt Nam

Tóm tắt: Trong các kết cấu bê tông khối lớn (BTKL), quá trình thủy hóa xi măng tạo ra lượng nhiệt lớn ở giai đoạn tuổi sớm. Do sự phân bố nhiệt độ khác nhau trong các vị trí của chúng dẫn đến chênh lệch nhiệt độ đáng kể giữa tâm và bề mặt khối bê tông. Khi chênh lệch nhiệt độ giữa các vị trí của kết cấu vượt quá chênh lệch nhiệt độ cho phép thì sẽ xuất hiện các vết nứt nhiệt. Do vậy, bài báo trình bày sự phát triển của trường nhiệt độ trong kết cấu BTKL với hai loại hỗn hợp bê tông khác nhau M_1 và M_2 . Cấp phối M_1 bao gồm 100% hàm lượng xi măng Portland thông thường và cấp phối M_2 bao gồm 65% xi măng Portland thông thường và 35% tro bay. Ngoài ra, bằng phương pháp phần tử hữu hạn đã khảo sát ảnh hưởng của nhiệt độ ban đầu của hỗn hợp bê tông (M_1, M_2) đến trường nhiệt độ trong kết cấu bê tông. Các kết quả nghiên cứu có thể được sử dụng để giảm nguy cơ hình thành vết nứt nhiệt trong kết cấu BTKL.

Từ khóa: Sự hình thành vết nứt; trường nhiệt độ; cường độ kéo; cường độ nén; nhiệt độ lớn nhất.

Received: 12/09/2022; Revised: 05/12/2022; Accepted for publication: 30/12/2022

